

# Epipole and fundamental matrix estimation using virtual parallax\*

B. Boufama

R. Mohr

LIFIA-INRIA

46 Av. Félix Viallet,

F- 38031 Grenoble Cédex, France

## Abstract

*This paper addresses the problem of computing the fundamental matrix which describes a geometric relationship between a pair of stereo images: the epipolar geometry. We propose here a novel method based on virtual parallax. Instead of computing directly the  $3 \times 3$  fundamental matrix, we compute a homography with one epipole position, and show that this is equivalent to compute the fundamental matrix. Simple equations are derived by reducing the number of parameters to estimate. As a consequence, we obtain an accurate fundamental matrix of rank two with a stable linear computation. Experiments with simulated and real images validate our method and clearly show the improvement over the existing methods.*

## 1 Introduction

Two images of the same rigid scene, taken from two different viewpoints, are related by the so-called *epipolar transformation*, also called *epipolar geometry* which has been described in publications too numerous to list here (see for example [2, 3, 6, 8]). In the uncalibrated case, i.e. when the images are obtained with uncalibrated cameras, the epipolar geometry is the only information we can get from point matches.

The epipolar geometry is used in particular for

- 3D reconstruction: The epipolar geometry is used for 3D reconstruction from stereo images [1, 3, 11]. In particular knowing the epipolar geometry of a pair of stereo images is equivalent to the knowledge of projective reconstruction [4].
- camera calibration: Camera self-calibration [7, 9] is a recent topic which aims to calibrate cameras only from point correspondances. If the feasibility has been shown, work still remain to be done to have robust methods in the field.
- matching and tracking: Once this geometry is computed, it reduces drastically the complexity of the matching between two images as the corresponding points lie on a line.
- motion segmentation: Rigidity might be violated in part of the image, it can be detected by violation of the epipolar constraint[12].

---

\*The reasearch described in this paper has been partially supported by Esprit Bra project Viva

This paper presents a new method for computing the epipolar geometry from point matches. It is based on the computation of the homography between a virtual plane and the images and detecting the parallax of points which do not belong to this plane. Beside of its elegance, the solution presented allows to express the epipolar geometry with a minimal number of unknowns and allows directly to express the fundamental matrix as a rank two matrix. This leads to simple and stable computation giving very accurate results. Furthermore, it degenerates gracefully in case of planar scenes, providing in such a case the homography between the two images.

The rest of this paper is organized as follows: in next section we present the basis of the epipolar geometry, the notation together with a brief description of the existing methods. Section 2 shows the geometric aspect of the relation between virtual parallax and epipolar geometry. In section 4 we present our method to solve for the epipole and the plane homography between the two images, we show that the fundamental matrix  $F$  is simply the product of an antisymmetrical matrix with a homography matrix and  $F$  is of rank two by construction. The experimental results are presented in section 5.

## 2 Basic properties and existing methods to compute $F$

Let two images be taken by two cameras by linear projection, as shown on Figure 1. Let  $O$  and  $O'$  be the two projection centers of the two images which will be called in the following: first and second image respectively. The point  $O$  projects to the point  $e'$  in the second image, and the point  $O'$  projects to the point  $e$  in the first image. The two points  $e$  and  $e'$  are the epipoles and the lines through  $e$  and  $e'$  are the epipolar lines. Let a space point  $P$  be projected on  $p$  and  $p'$  respectively in the first and the second image. The plane defined by the three points  $P$ ,  $O$  and  $O'$  is the epipolar plane, it contains the two points  $p$  and  $p'$ . The projections of this plane onto the first and the second image are respectively the epipolar lines  $(e, p)$  and  $(e', p')$ . We can see from Figure 1 that the relation between the epipolar lines in the first image and the epipolar lines in the second image is a homography of lines. This homography is the epipolar transformation which relates a pair of stereo images. The first method to compute the epipolar geometry from point matches was proposed by Hesse[5], and later clarified

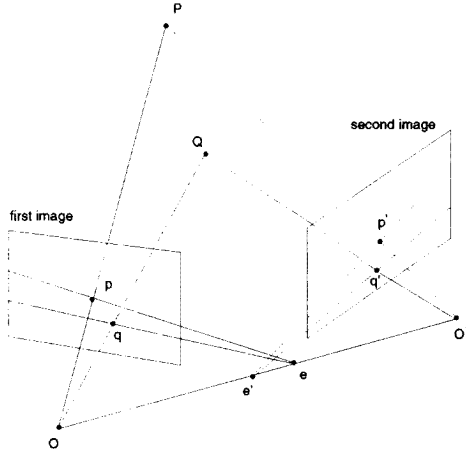


Figure 1: A space point  $P$  defines the epipolar plane  $OPO'$  which intersects the two image planes in two lines  $(ep)$  and  $(e'p')$ : the epipolar lines.

and summarised by Sturm [13]. The latter proposes an algorithm to compute the epipoles and the epipolar transformation compatible with 7 matched points in a general configuration. However, this algorithm is only of theoretical interest, it doesn't consider the case of noisy data. Furthermore, even if redundant data is used, i.e. more than 8 matched points are used and noise is considered, the computation is very unstable leading very often to incorrect results [6].

The most common way to describe the epipolar geometry is by means of a  $3 \times 3$  matrix called the *fundamental matrix*. This matrix, usually noted  $F$ , contains the geometric information which relates a couple of stereo images. For a point  $p$  given by its homogeneous coordinates in the first image, the corresponding epipolar line  $l_p$  in the second image is given by :

$$l_p = Fp$$

$l_p$  is a vector containing the coefficients of the line.

If in the second image  $p'$  is the corresponding point to  $p$  then  $p'$  must belong to  $l_p$ , this can be written as

$$p'^T Fp = 0 \quad (1)$$

$F$  is homogeneous and is of rank two [8], it has seven independent parameters.

The most used methods to compute  $F$  are based on the above equation. A brief description of these methods follows.

Let's assume that points have been matched in the 2 images. When using (1), each couple of match points  $(p, p')$  gives rise to a linear homogeneous equation in the nine unknowns of  $F$ . Since  $F$  can only be defined up to a scale factor, it has 8 independent parameters. So  $F$  can be computed with 8 matched points in the 2 images. When more than 8 matches are given, a linear least square method can be used to compute  $F$ . However, such method is very sensitive to noise as shown by the experiments of Luong [6]. Furthermore,

there is no way to ensure the rank property of  $F$  when using only linear equations.

In practice,  $F$  computed using equations (1) is not correct, particularly when the epipoles are far from the center of the image. This is due to the parametrization of the epipolar transformation which is represented here by 9 parameters instead of 7. In particular,  $F$  obtained by solving the linear equations (1) is not of rank 2 when real data are used.

To overcome this problem, a nonlinear minimization with the rank constraint is used, the following criterion is often used (see [6] for more details) :

$$\min \sum_i \{d^2(p'_i, Fp_i) + d^2(p_i, F^T p'_i)\} \quad (2)$$

where  $d^2(p'_i, Fp_i)$  is the square distance of the image point  $p'_i$  to its corresponding epipolar line  $(Fp_i)$ .

Therefore,  $F$  is computed in two steps: by using the linear criterion (1), a solution for  $F$  is computed with a linear least square method, this first solution is used as a starting point for a nonlinear minimization based on (2). In the following, these 2 steps are called respectively the linear and the nonlinear algorithm.

This algorithm has one major weakness, the convergence of the nonlinear method to the correct solution for  $F$  depends on the initialization provided by the linear solution. The latter gives very often a false solution which sometimes leads to a local minimum for the function defined in (2). It results into more iterations for the nonlinear step, and in some cases the method converges to a local minimum. An example illustrating this problem is presented in section 5.

### 3 Epipolar geometry, virtual parallax

Let  $\Pi_{123}$  be a plane defined by 3 space points  $P_1, P_2$  and  $P_3$ ; and let's consider 2 other space points  $P_4$  and  $P$  not belonging to  $\Pi_{123}$ . These points are observed by 2 cameras providing 2 images called in the following first and second image (see Figure 2).

The line  $(OP_4)$  intersects  $\Pi_{123}$  in the point  $Q_4$  (Figure 2). In the first image both  $P_4$  and  $Q_4$  project onto the same image point  $p_4$ . However, in the second image they project onto 2 different points  $p'_4$  and  $q'_4$  (parallax effect). This is always true when the motion between the two cameras has a non null translation component. In a similar way, the two space points  $P$  and  $Q$  project on the same image point  $p$  in the first image and on 2 points  $p'$  and  $q'$  in the second image.

In the second image, the 2 image lines  $(p'_4 q'_4)$  and  $(p' q')$  are the projections of the two space lines  $(OP_4)$  and  $(OP)$  respectively. It's clear that  $(p'_4 q'_4)$  and  $(p' q')$  are the epipolar lines corresponding to the two points  $p_4$  and  $p$  of the first image. Hence,  $(p'_4 q'_4)$  and  $(p' q')$  intersect in the epipole  $e'$  (see figure 2). Unfortunately, the locations of  $q'_4$  and  $q'$  are not given since these points are the projection of virtual points. If by some means the projection of such points can be located in the second image, the problem would be solved. For example if 4 space points were known to be coplanar, then, it would be possible to compute the plane homography between the two images, this homography

would give the projection of these virtual points in the second image. In such case, the epipolar geometry could be computed with only 6 match points where exactly 4 of them are coplanar [10]. However, this a priori knowledge is not available: the next section provides the solution.

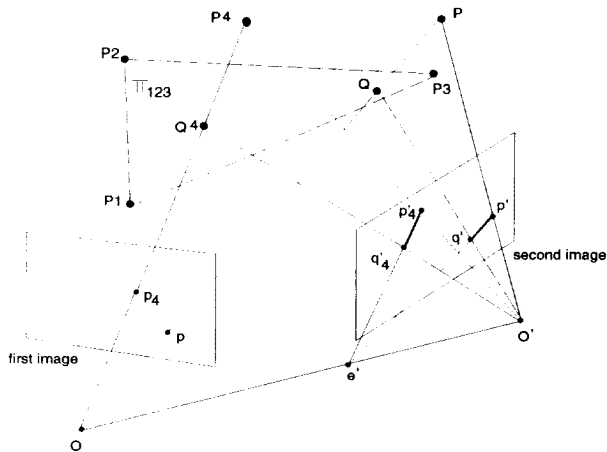


Figure 2: Epipolar geometry and virtual parallax

#### 4 Epipole and fundamental matrix estimation

We propose here a method to compute the fundamental matrix given match points in 2 images. We use in this section the same notations as in Figure 2.

Consider a space point  $P$ , and let the virtual point  $Q$  be the intersection of the plane  $\Pi_{123}$  with the line  $(OP)$ . Suppose we have a means which enables us to find for each space point  $P$  the projection  $q'$  of the corresponding virtual point  $Q$  in the second image. If in addition the epipole  $e'$  in the second image is known then to a point  $p$  in the first image corresponds an epipolar line in the second image given by  $(e'q')$ . The reverse is also true if we exchange the 2 images. This is equivalent to the fundamental matrix.

Let  $H$  and  $H'$  be the 2 plane homographies corresponding to the projections of  $\Pi_{123}$  onto  $\Pi$  and  $\Pi'$  in the first and the second image respectively where :

$$\Pi = H(\Pi_{123}) \text{ and } \Pi' = H'(\Pi_{123})$$

As nonsingular homographies are invertible, there exists a plane homography  $K$  between  $\Pi$  and  $\Pi'$  such that  $K = H'H^{-1}$ , where  $H^{-1}$  is the inverse of  $H$ .

We have the following relation :

$$\forall p \in \Pi, K(p) = q' \text{ with } q' \in \Pi'$$

Where, according to Figure 2,  $p$  is the projection in the first image of the point  $P$  and  $q'$  is the projection in the second image of the virtual point  $Q$ .

Let the homography  $K$  be described by a  $3 \times 3$  matrix  $C$ . By using homogeneous coordinates for the image points we have :

$$\forall p \in \Pi, Cp = \lambda q' \quad (3)$$

where  $\lambda$  is an unknown scale factor.

Note that  $q'$  could be the projection of a real point if it belongs to  $\Pi_{123}$ . In particular, we have :

$$Cp_i = \lambda_i p'_i, \quad i = 1 \dots 3 \quad (4)$$

where  $p_i$  and  $p'_i$  are respectively the projections of  $P_i$  in the first and the second image.

For each couple  $(p_i, p'_i)$ , the above relation gives rise to 2 independent linear equations in the nine unknown coefficients of  $C$ . Thus  $P_1, P_2$  and  $P_3$  introduce 6 linear equations. Since  $C$  is homogeneous, it has only 8 independent parameters and we can write it as depending on only 2 parameters (see next paragraph).

##### 4.1 Simple expression for $C$

Let's make 2 choices of coordinate systems in the 2 image planes by choosing a projective basis such that :

$$\begin{aligned} p_1 &= (0, 0, 1)^T & p'_1 &= (0, 0, 1)^T \\ p_2 &= (1, 0, 0)^T & p'_2 &= (1, 0, 0)^T \\ p_3 &= (0, 1, 0)^T & p'_3 &= (0, 1, 0)^T \\ p_0 &= (1, 1, 1)^T & p'_0 &= (1, 1, 1)^T \end{aligned}$$

$(p_i, p'_i)$ ,  $i = 1 \dots 3$  are the projections on the 2 images of  $P_1, P_2$  and  $P_3$ ;  $(p_0, p'_0)$  is a couple of matched points such that no 3 of these 4 points are collinear.

Under such choice of coordinate systems and after using relation (4) for the three couples  $(p_i, p'_i)$ ,  $i = 1 \dots 3$ , the expression of  $C$  can be written as :

$$C = \begin{pmatrix} \alpha & 0 & 0 \\ 0 & \beta & 0 \\ 0 & 0 & 1 \end{pmatrix} \quad (5)$$

In fact, the above matrix has 3 parameters, but only two of them are independent. Furthermore, these 3 parameters can not be null for a nonsingular homography. Since our homography maps a plane onto a plane  $C$  does not describe a singular homography. Thus, we can fix one of the 3 parameters of  $C$ . For our case we set it equal to 1 (the last element of  $C$ ).

Note that up to now, we only made use of 3 matched points in the two images.

##### 4.2 Basic equation

Let's suppose here that  $C$  has the form given in (5) and any couple of matched points  $(p, p')$  are given by their homogeneous coordinates vectors  $(x, y, t)^T$  and  $(x', y', t')^T$  respectively. By using the relation (3) and the simple form of  $C$  given in (5), the homogeneous coordinates of the projection  $q'$  of the virtual point  $Q$  in the second image are given by :

$$Cp = \lambda q' = \lambda(\alpha x, \beta y, t)^T \quad (6)$$

where only  $\alpha$  and  $\beta$  are unknown here.

Let  $(e'_x, e'_y, e'_t)^T$  be the unknown homogeneous coordinates of the epipole  $e'$  in the second image. It is clear from Figure 2 that in the second image  $q'$  belongs to the line  $(e'p')$  which is the epipolar line corresponding to  $p$ . This can be written as :

$$(e' \times p') \cdot q' = 0 \quad (7)$$

where  $\times$  is the cross product and  $\cdot$  the scalar product.

$(e' \times p')$  is a vector of dimension 3, the elements of this vector are the 3 coefficients of the line  $(e'p')$ .

By expanding (7) and using the coordinates of  $q'$  given in (6) we obtain the following equation:

$$(e'_t y' - t' e'_y) \alpha x + (t' e'_x - e'_t x') \beta y + (e'_y x' - y' e'_x) t = 0 \quad (8)$$

Equation (8) has 5 unknowns:  $\alpha$ ,  $\beta$ ,  $e'_x$ ,  $e'_y$  and  $e'_t$ . Since  $(e'_x, e'_y, e'_t)^T$  are the homogeneous coordinates of  $e'$ , only 2 of these 3 coordinates are independent. Consequently, we have only 4 independent unknowns in the equation above. So, in addition to the 3 couples of matched points in the two images are necessary to solve for the 4 independent unknowns of equation (8). Thus, at least 7 matched points are necessary to solve for the plane homography and the epipole in one image. However, the above equation is nonlinear.

Let's distinguish the unknowns by using the following notations:

$$\alpha = X_1, \quad \beta = X_2, \quad e'_x = X_3, \quad e'_y = X_4 \quad (9)$$

and  $e'_t = X_5$ .

and let's use the following notations:

$$a_i = x_i y'_i, \quad b_i = -x_i t'_i, \quad c_i = y_i t'_i, \quad d_i = -y_i x'_i, \quad (10)$$

$e_i = t_i x'_i$  and  $f_i = -t_i y'_i$

where  $(x_i, y_i, t_i)^T$  and  $(x'_i, y'_i, t'_i)^T$  are the homogeneous coordinates of image points  $p_i$  and  $p'_i$  respectively.

For each couple of matched point  $(p_i, p'_i)$ , the equation (8) can now be written as:

$$a_i X_1 X_5 + b_i X_1 X_4 + c_i X_2 X_3 + d_i X_2 X_5 + e_i X_4 + f_i X_3 = 0 \quad (11)$$

Note that the coefficients  $a_i$ ,  $b_i$ ,  $c_i$ ,  $d_i$ ,  $e_i$  and  $f_i$  can not be zero all together.

The above equation is the basic equation of the epipolar geometry based on virtual parallax, where we have, 4 independent unknowns describing a problem depending exactly on 4 independent parameters.

Equation (11) is nonlinear, but by using the following unknowns transformation:

$$\begin{aligned} X_1 X_5 &= V1, & X_1 X_4 &= V2, & X_2 X_3 &= V3, \\ X_2 X_5 &= V4, & X_4 &= V5 \text{ and } X_3 &= V6 \end{aligned} \quad (12)$$

Equation (11) becomes;

$$a_i V_1 + b_i V_2 + c_i V_3 + d_i V_4 + e_i V_5 + f_i V_6 = 0. \quad (13)$$

The above equation is linear, but with one more parameter. So at least 5 independent equations must be used to solve for the unknowns  $V_i$ . As a consequence, a linear computation for the epipole ( $e'$ ) and the plane homography ( $C$ ) is possible when 8 couples of matched points are given. This linear computation can be followed by a nonlinear one using equation (11) to ensure the use of a minimal number of parameters.

### 4.3 Number of solutions with 7 points

In this paragraph we show that 3 solutions for the epipole are compatible with 7 matched points in 2 images. This result was established by Sturm [13], however the proof given here is must simpler.

Suppose we have 7 couples of matched points between the first and the second image, 3 of them are used to simplify the expressions of the plane homography and the remaining 4 couples are used to solve for the 4 independent unknowns of equation (11). The epipole  $e' = (e'_x, e'_y, e'_t)^T$  has only 2 independent coordinates, for the simplicity of the proof we assume here that the first coordinate of  $e'$  is non zero and therefore it can be set to 1 transforming equation (11) to:

$$a_i X_1 X_5 + b_i X_1 X_4 + c_i X_2 + d_i X_2 X_5 + e_i X_4 + f_i = 0 \quad (14)$$

In theory, a solution exists for the unknowns  $X_1 \dots X_4$  when using 4 equations of type (14).

By using (12) the above equation becomes:

$$a_i V_1 + b_i V_2 + c_i V_3 + d_i V_4 + e_i V_5 + f_i = 0. \quad (15)$$

Using equation (15) for 4 couples of matched points (different from the 3 couples used to simplify  $C$ ), it is possible to solve for  $V_1 \dots V_4$  as a function of  $V_5$ .

The solution of (15) has the form:

$$V_j = A_j V_5 + B_j \quad j = 1 \dots 4 \quad (16)$$

where  $A_j$  and  $B_j$  are known coefficients, they depend on the constants  $a_i$ ,  $b_i$ ,  $c_i$ ,  $d_i$ ,  $e_i$  and  $f_i$ .

Replacing each  $V_j$  by its expression in (12) then using (16) and after simple algebraic manipulations we obtain the following cubic equation in the unknown  $X_4$ :

$$\begin{aligned} A_1 A_3 X_4^3 + (A_3 B_1 + B_3 A_1 - A_2 A_4) X_4^2 + \\ (B_1 B_3 - A_2 B_4 - B_2 A_4) X_4 - B_2 B_4 = 0 \end{aligned}$$

The above equation has 3 roots, this shows that up to 3 solutions compatible with 7 couples of matched points exist for the epipole position. Hence, we retrieve in a simpler way the result demonstrated by Sturm [13, 2]. When more than 7 matched points are available, the unicity of the solution can be ensured.

We have not computed the fundamental matrix yet, next section shows how it can be deduced from the knowledge of one epipole and a plane homography.

### 4.4 Fundamental matrix

Suppose we are given 8 matched points. This enables us (paragraph 4.2) to compute the epipole coordinates  $(e'_x, e'_y, e'_t)^T$  in the second image and the matrix  $C$  describing a plane homography between the first and the second image.

Let  $F$  be the unknown fundamental matrix.  $F$  is a  $3 \times 3$  matrix such that for each point  $p = (x, y, t)^T$  of the first image  $F$  associates the epipolar line  $l_p$  in the second image,  $l_p$  is given by  $(Fp)$ .

For the same point  $p$ , the epipolar line  $l_p$  can also be defined by the two points  $e'$  and  $q'$  ( $q'$  is the point obtained from  $p$  by the homography described by  $C$  as

shown in Figure 2). The equation of this line is given by  $(e' \times q')$ . By using relation (3), the equation of  $l_p$  becomes  $(e' \times (Cp))$  where :

$$e \times Cp = \begin{pmatrix} 0 & -\beta e'_t & e'_y \\ \alpha e'_t & 0 & -e'_x \\ -\alpha e'_y & \beta e'_x & 0 \end{pmatrix} \begin{pmatrix} x \\ y \\ t \end{pmatrix} \sim \begin{pmatrix} A_p \\ B_p \\ C_p \end{pmatrix}$$

From the above, it is clear that the fundamental matrix  $F$  is deduced directly from  $e'$  and  $C$  :

$$F = \begin{pmatrix} 0 & -e'_t & e'_y \\ e'_t & 0 & -e'_x \\ -e'_y & e'_x & 0 \end{pmatrix} \begin{pmatrix} \alpha & 0 & 0 \\ 0 & \beta & 0 \\ 0 & 0 & 1 \end{pmatrix} \quad (17)$$

$F$  defined from the above relation satisfies the criterion given in (1). Furthermore,  $F$  is by construction of rank 2. Consequently,  $F$  is a fundamental matrix relating two images.

As a consequence, with 8 matched points, a fundamental matrix  $F$  of rank 2 can be computed using only linear equations given by (13).

## 5 Experimental results

*Summary of our algorithm :*

Given at least 8 couples of matched points as input,

- select 3 points in the first image and use them with a fourth point as a projective basis which defines a new coordinate system in the image (in practice, the points are chosen largely spread in the image). Similarly, define a new coordinate system in the second image.
- use the remaining matched points to solve for the unknowns by using the linear equations given in (13). This step is called the linear algorithm.
- when a nonlinear step is needed, the solution obtained by the linear algorithm is used as a starting point for a nonlinear computations. This second step is based on the nonlinear equations (11). This step is called the nonlinear algorithm.

To compute the quality of the computed fundamental matrix  $F$  we used the following formula :

$$Q_F = \frac{\sum_{i=1}^n d(p'_i, Fp_i) + d(p_i, F^T p'_i)}{2n} \quad (18)$$

where  $(p_i, p'_i)$ ,  $i = 1 \dots n$ , are the  $n$  couples of matched points and  $d$  is the point-to-line Euclidean distance expressed in pixels.  $Q_F$  is called in the remaining the quality factor of  $F$ .

### 5.1 Experiments with simulated images

We simulated a scene consisting of 60 points with a  $40cm \times 30cm \times 30cm$  volume placed at 1 meter from the virtual camera. Two sets of experiments have been carried out, where  $F$  is computed using our algorithm :

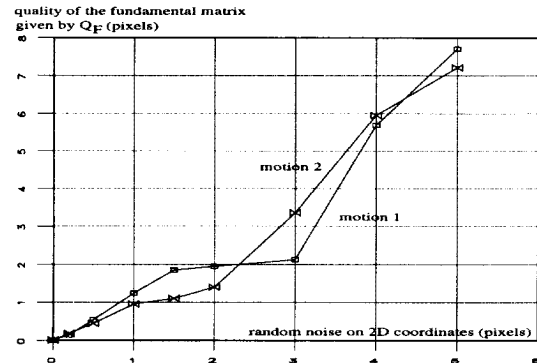


Figure 3: The stability of the method for 2 different motions using 60 points.

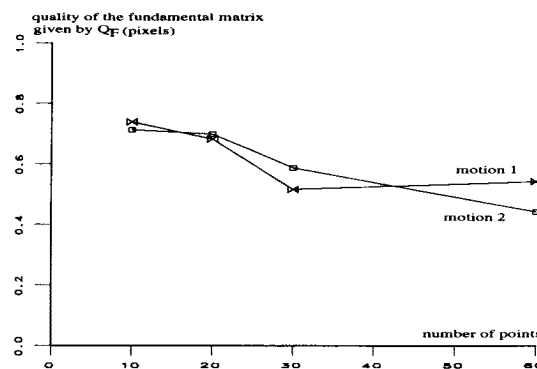


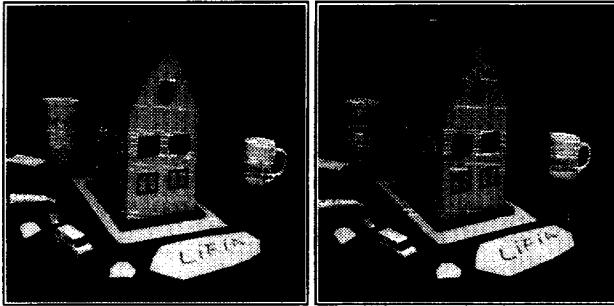
Figure 4: The stability of the method for 2 different motions when the number of points decreases.

1. Two different motions for the camera have been simulated: one motion is mainly composed by a lateral translation and the other one is mainly composed by a translation toward the scene. For each motion, the fundamental matrix is computed several times by adding a uniform noise of different magnitudes. All points were used here to compute  $F$ . The results are shown on Figure 3.
2. The second set of experiments consists of performing the former experiments where instead of changing noise magnitude we changed the number of matched points used to compute  $F$ . Here, the noise magnitude is kept equal to 0.5 pixel. The results are shown on Figure 4.

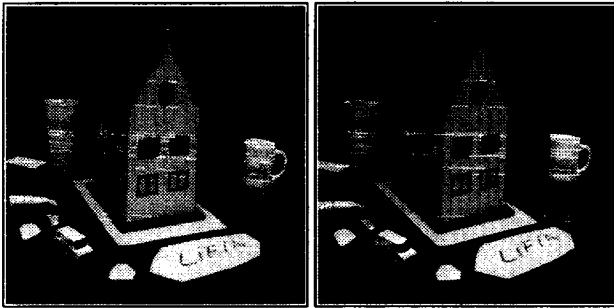
The results of the above experiments show the stability of the method for 2 different camera movements. As shown in Figure 3 and Figure 4, there is no significant effect on the computed epipolar geometry with the 2 different motions even when using less points.

### 5.2 Experiments with real images

We used 2 different scenes to test our method, and we compared our results with those obtained by the existing method based on (1).



Our linear algorithm result,  $Q_F = 0.81$  pixels



Our nonlinear algorithm result,  $Q_F = 0.43$  pixels

Figure 5: The camera movement is mainly a lateral translation, 49 points are used here.

1. An indoor scene, the house (figure 5): the motion between the images is mainly a lateral translation.
2. An outdoor scene, Bayard (figure 6): the motion between the 2 images is mainly a translation.

When using the nonlinear step of our method, the iterations number was always less than 10.

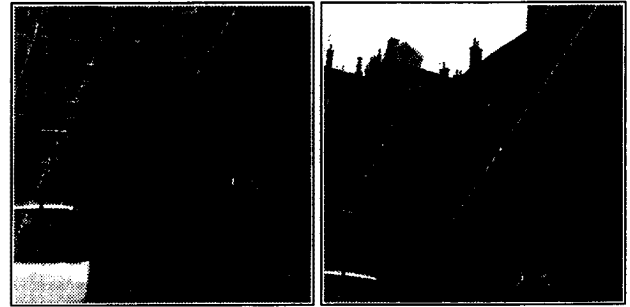
### 5.2.1 Comparison with the existing method

Epipolar geometry using the existing method based on (1) and (2) is computed for the real scenes :

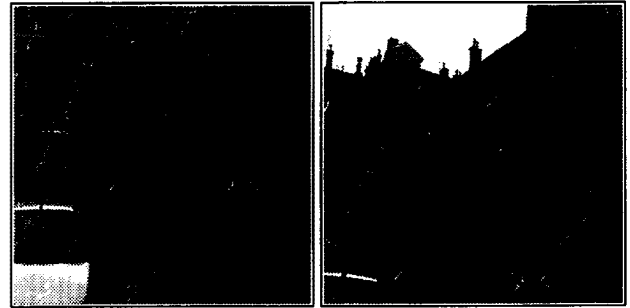
1. the house scene (figure 7) : when using only linear computation based on equations (1) the result is very far from the correct solution (compare with the result of our linear method shown on figure 5). Using the nonlinear computation based on (2), we obtained the correct solution after 72 iterations.
2. Bayard scene (figure 8) : when using only linear computation the result is false, it corresponds to a local minima for the function (2). Using this solution as initialization for the nonlinear computation did not get out from this local minima.

## 6 Conclusion

The epipolar geometry relating a pair of stereo images can be computed from pixel correspondences.

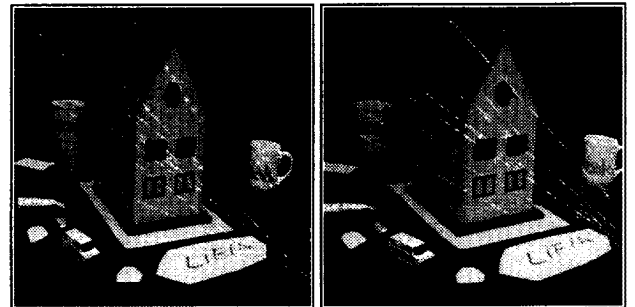


Our linear algorithm result,  $Q_F = 0.47$  pixels

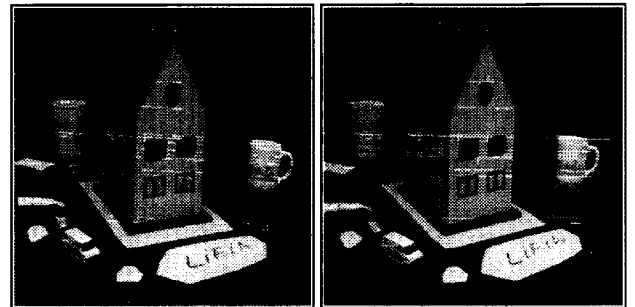


Our nonlinear algorithm result,  $Q_F = 0.26$  pixels

Figure 6: The camera movement is mainly a translation, 25 points are used here.

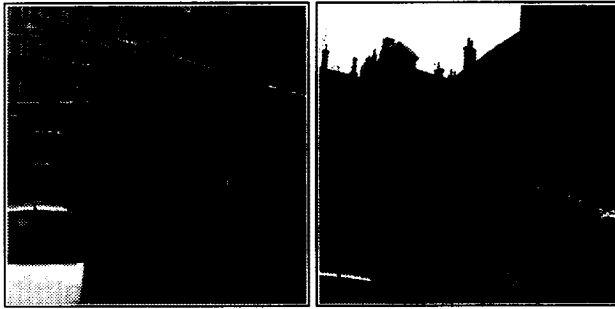


Standard linear algorithm result,  $Q_F = 3.22682$  pixels

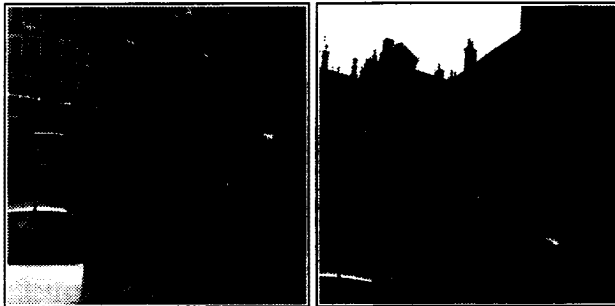


Standard nonlinear algorithm result,  $Q_F = 0.42$  pixels

Figure 7: The nonlinear algorithm has recovered the error of the linear algorithm.



Standard linear algorithm result,  $Q_F = 0.89$  pixels



Standard nonlinear algorithm result,  $Q_F = 0.66$  pixels

Figure 8: The nonlinear method fails in recovering the correct epipolar geometry, being trapped in a local minimum (compare with Figure 6).

The most common way to represent the epipolar geometry is the use of the fundamental matrix  $F$ , that is a homogeneous  $3 \times 3$  matrix of rank 2.

The linear computation of  $F$  in the existing methods does not ensure the rank property. A nonlinear step is usually used and its convergence to the correct solution depends on its initialization.

We proposed in this paper a novel method to compute the epipolar geometry based on virtual parallax. Unlike the existing method which estimates the fundamental matrix, we presented here another parametrisation for the epipolar geometry. The method consists of estimating an epipole position and a 2D homography. A choice of coordinate systems in the images allowed us to reduce the number of parameters to estimate. This simplification leads to more stable computation. Furthermore, in our formulation the rank constraint is implicit because the fundamental matrix  $F$  is simply the product of an antisymmetrical matrix by the homography induced by the mapping of the virtual plane. Finally in the case of planar scenes, the epipolar geometry computation we proposed gracefully degenerates into an homography between the two image planes allowing matching for instance. Experimental results on real outdoor and indoor scenes prove the accuracy than can be obtained (less than  $1/2$  pixel).

## References

- [1] O. Faugeras. What can be seen in three dimensions with an uncalibrated stereo rig? In G. Sandini, editor, *Proceedings of the 2nd European Conference on Computer Vision, Santa Margherita Ligure, Italy*, pages 563–578. Springer-Verlag, May 1992.
- [2] O.D. Faugeras, Q.T. Luong, and S.J. Maybank. Camera Self-Calibration: Theory and Experiments. In G. Sandini, editor, *Proceedings of the 2nd European Conference on Computer Vision, Santa Margherita Ligure, Italy*, pages 321–334. Springer-Verlag, May 1992.
- [3] R. Hartley, R. Gupta, and T. Chang. Stereo from uncalibrated cameras. In *Proceedings of the Conference on Computer Vision and Pattern Recognition, Urbana-Champaign, Illinois, USA*, pages 761–764, 1992.
- [4] R.I. Hartley. Euclidean reconstruction from uncalibrated views. In *Proceeding of the DARPA-ESPRIT workshop on Applications of Invariants in Computer Vision, Azores, Portugal*, pages 187–202, October 1993.
- [5] O. Hesse. Die cubische Gleichung, von welcher die Lösung des Problems der Homographie von M. Chasles abhängt. *J. reine angew. Math.*, (62):188–192, 1863.
- [6] Q.T. Luong. *Matrice Fondamentale et Autocalibration en Vision par Ordinateur*. Thèse de doctorat, Université de Paris-Sud, Orsay, France, December 1992.
- [7] Q.T. Luong and O.D. Faugeras. Self-calibration of a camera using multiple images. In *Proceedings of the 11th International Conference on Pattern Recognition, The Hag, Netherland*, pages 9–12, 1992.
- [8] S. Maybank. *Theory of Reconstruction from Image Motion*. Springer-Verlag, 1993.
- [9] S.J. Maybank and O.D. Faugeras. A theory of self calibration of a moving camera. *International Journal of Computer Vision*, 8(2):123–151, 1992.
- [10] R. Mohr. Projective geometry and computer vision. In C.H. Chen, L.F. Pau, and S.P. Wang, editors, *Handbook of Pattern Recognition and Computer Vision*. World Scientific Pub. Co., 1993.
- [11] A. Shashua. Projective Structure from Two Uncalibrated Images : Structure from Motion and Recognition. Technical Report A.I. Memo No. 1363, Massachusetts Institute of Technology, September 1992.
- [12] D. Sinclair, B. Boufama, and R. Mohr. Independent motion segmentation and collision prediction for road vehicules. In *Proceedings of the Conference on Computer Vision and Pattern Recognition, Seattle, Washington, USA*, pages 958–961, June 1994.
- [13] R. Sturm. Das Problem der Projektivität und seine Anwendung auf die Flächen zweiten Grades. *Math. Ann.*, 1:533–574, 1869.